Hindawi
Modelling and Simulation in Engineering
Volume 2020, Article ID 8855192, 12 pages
https://doi.org/10.1155/2020/8855192

Research Article

Development of Automatic Equipment for Washing and Nondestructive Inspection of Stud Bolt

H. S. Kwak

School of Mechanical and Automotive Engineering, Youngsan University, 50510, Republic of Korea

Correspondence should be addressed to H. S. Kwak; hyoseo0403@ysu.ac.kr

Received 7 July 2020; Revised 22 October 2020; Accepted 26 November 2020; Published 28 December 2020

Academic Editor: Gaetano Sequenzia

Low-pressure steam turbines in a power plant are required to operate at high temperatures and under high pressures to achieve better energy utilization and better performance. Higher operating temperatures accelerate the rate of oxidation and sludge formation, so the steam turbine is periodically inspected including strict examination of the stud bolts, and it is necessary to clean the bolts by removing sludge from their screw threads. In the conventional cleaning process, the sludge has been removed by manual cleaning, which is labor-intensive and time-consuming. Therefore, this study developed automatic equipment for washing and nondestructive inspection of stud bolts using theoretical analysis and finite element analysis (FEA). An optimal clamp load to prevent sliding of the roller was calculated, and a structural analysis of the equipment under operating conditions was conducted. An optimal washing condition to maximize cleaning efficiency was proposed using design of the experiment and verified by performing washing test of prototype.

1. Introduction

To increase power generation efficiency, low-pressure steam turbines used in a nuclear power plant had been developed to be able to operate at higher temperature and high-pressure steam conditions. Turbine oil operating in high-temperature environments is exposed to air and catalytic metals. Fast flow rates and short reservoir residence times provide more opportunities for air and oil to interact and react, and the gas temperature (and hence particle temperature) governs the softening and viscosity of the particle, while the surface temperature governs the stickiness of the deposit [1]. Therefore, higher operating temperatures accelerate the rate of oxidation and thermal degradation of the turbine oil, which means that sludge formation occurs more rapidly at higher temperatures [2]. Using a compressor fluid creates and accumulates sludge composed of oxidized steel and oxidized copper, which can lead to a safety problem, possibly even an explosive situation if coupled with overheating. This will occur if sufficient quantities of carbon and sludge are formed to cause the valves to stick pent. It can lead to an increase in bearing temperatures, stuck valves, and blocked filters, which can cause unplanned downtime and lower productivity [3–5]. One of the greatest problems encountered is that sludge sticks on stud bolts in the steam turbine shown in Figure 1. Steam turbine and related equipment in power plants are periodically inspected. The inspection includes not only the disassembling of the machine parts but also the strict examination of the stud bolts, and it is necessary to clean the bolts by removing sludge from their screw threads and polishing them. When the bolts are removed to enable the inspection or replacement of any machine part, it is also usual to clean the screw threads of the bolts. In the conventional cleaning process, the sludge has been removed by manual cleaning, which is labor-intensive and time-consuming and does not completely clean the threads. Furthermore, the clamp load applied to the bolts was inaccurately determined by worker's experience. Therefore, automatic equipment for washing the stud bolt has been required in the actual field.

In the previous studies related to cleaning system for any type of bolt used in a power plant, Muraguchi developed a device which can clean a bolt efficiently and is easy to use without vibrating. The cleaning comprises a sleeve having an open end, a rotor provided in the sleeve substantially

Figure 1: Stud bolt used in a low-pressure turbine of a power plant.

coaxially and brushes brought into rubbing contact with the surface of the bolt by rotating the rotor in which the bolt is inserted. The cleaning operation is performed in the sleeve which forms an enclosed space to the exterior [6]. Linna et al. developed the bolt automatic cleaning technology to enhance the automation degree of bolt cleaning in the reactor pressure vessel. The key technology for the bolt automatic cleaning and the 3D design technology are used to simulate the cleaning process. The test results show that the bolt cleaning equipment is of high reliability [7]. Shindo et al. developed a remote-controlled stud bolt handling device for a reactor pressure vessel used in general nuclear power plant, in which the equipment for stud bolt cleaning, nut handling, and stud bolt tensioning has been combined. A considerable shortening of working hours and labor saving was accomplished [8]. Saurer, Muraguchi, and Gibson Sr. presented patents on cleaning devices for the bolt, respectively [9–11]. Xie et al. developed a model for optimizing the flue gas cleaning systems using computational fluid dynamics to simulate the flue gas cleaning by the spray dryer of a waste incineration power plant. The model was used to evaluate the removal efficiencies of HCl and SO_2 of the gas cleaning system with an error of less than 5% between simulated results and measured values [12]. Lee et al. proposed a spray slurry nozzle to reduce the slurry consumption and increase the material removal rate (MRR) in SiO_2 chemical mechanical planarization (CMP). Adopting the spray slurry nozzle in CMP process provides a higher friction force and shorter process time than the normal tube-type slurry nozzle, which reduces the slurry and electricity consumption [13]. In the previous studies related to the sliding and friction of rubberlike material, Mofidi et al. researched rubber sliding friction on hard lubricated surface and found that short-wavelength roughness was the dominant contribution to rubber friction. Sliding friction is mainly due to the viscoelastic deformations of the rubber by the counterface surface asperities [14].

To overcome the existing problems, this study developed automatic equipment for washing stud bolts using theoretical analysis and finite element analysis (FEA). An optimal clamp load to prevent sliding of roller was calculated, and structural analysis of the equipment under operating conditions was conducted. Optimal washing conditions to maximize cleaning efficiency were proposed using the design of experiment and verified by performing washing test of prototype. Furthermore, the washing part and the nondestructive part were combined into one integrated equipment, and this reduces installation space and improves work efficiency and convenience. The methodology (process, material, and software) for the development of the automatic machine is described in Figure 2.

2. Design of the Automatic Equipment

This study developed the automatic equipment for washing and nondestructive inspection of stud bolts consisting of driving rollers, driven rollers, a clamp, a brush, a shaft, and injection nozzles. It has four stages as shown in Figure 3. In step 1, the stud bolt is located on driving and driven rollers to move to the next stage, and then, a clamp comes down and presses the stud bolt down to prevent sliding. In step 2, a brush roller moves down until it contacts the stud bolt and cleans the sludge by a rotating motion with a constant set rotation speed. At the same time, each injection nozzle sprays washing liquid and air with set injection pressures, respectively, to remove the remaining sludge. When the cleaning process is completed, the brush and the clamp move up, and injection of washing liquid and air stops. In step 3, the stud bolt is transferred into a nondestructive inspection stage to conduct an eddy current test (ECT). The ECT is a nondestructive testing technology that provides the ability to electronically drive multiple eddy current coils, which are placed side by side in the same probe assembly. To detect defects such as cracks and corrosion, variations in the changing phases and magnitude of eddy currents are monitored by using a receiver coil. When an alternating current is passed through a conductor (copper coil), an alternating magnetic field is developed around the coil which contracts as the alternating current rises and falls. If the coil is then brought close to another electrical conductor, the fluctuating magnetic field surrounding the coil permeates the bolts and induces an eddy current to flow in the conductor. This eddy current, in turn, develops its magnetic field. This secondary magnetic field opposes the primary magnetic field. Any changes in the conductivity of the material being examined, such as near-surface defects or differences in thickness, will affect the magnitude of the eddy current. This change is detected using the detector coil, forming the basis of the eddy current testing inspection technique. The brushing process precedes the washing liquid and air spray process to achieve better accuracy of ECT. In step 4, the stud bolt is unloaded, and the configuration of the equipment is illustrated in Figure 4.

In the washing and nondestructive inspection stages, the stud bolt, which is located on the driving and driven rollers, is rotated by their rotating motion, and then, the clamp presses down on the stud bolt to prevent sliding, as shown in Figure 5. If the clamp load is too small or large, the stud bolt runs idle, which causes a reduction of washing efficiency. So, an optimal clamp load to prevent the stud bolt from sliding is calculated considering operating conditions.

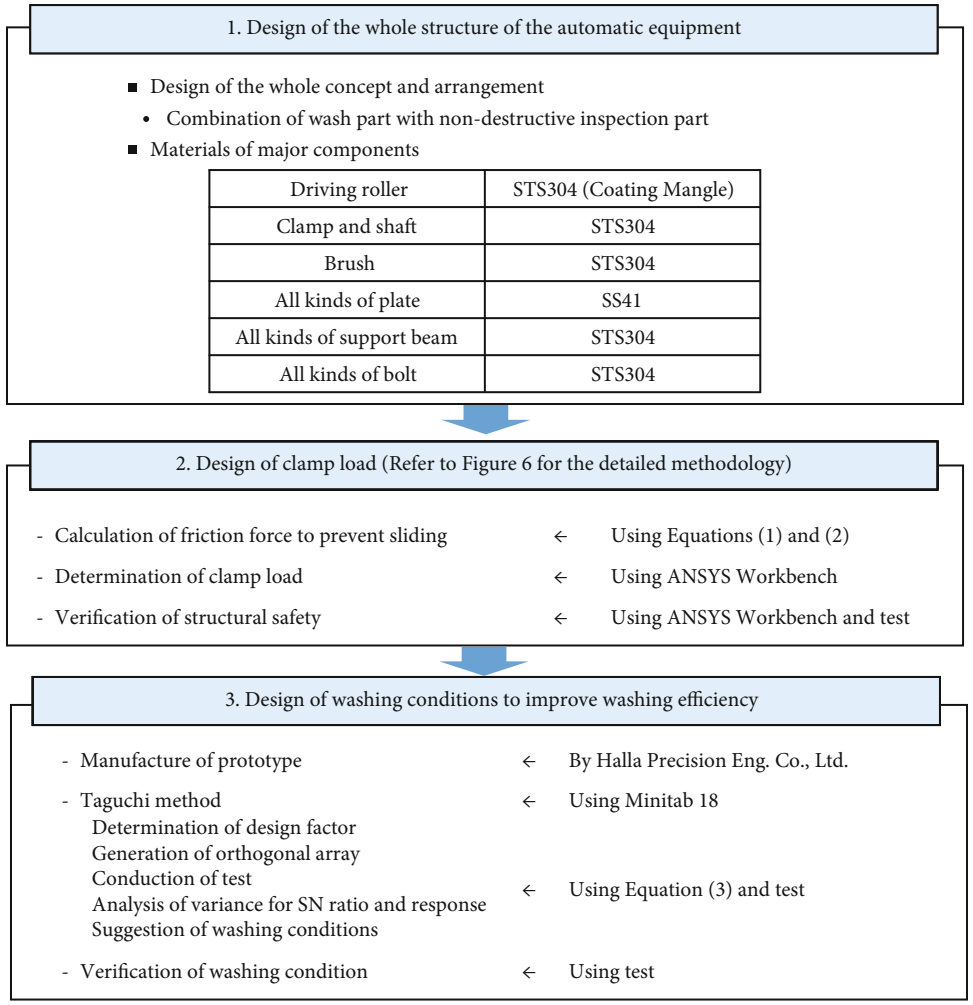

Figure 2: Methodology for the development of the automatic machine.

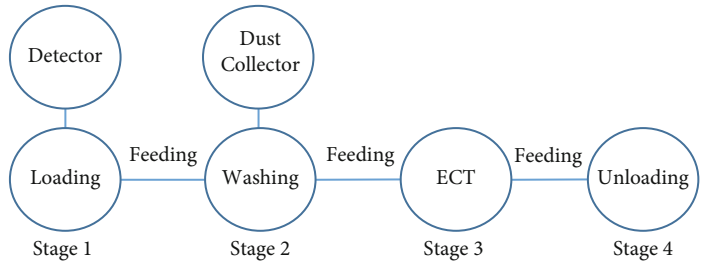

Figure 3: Process of equipment for washing and nondestructive inspection of stud bolt.

3. Design of Optimal Clamp Load

The optimal clamp load to prevent sliding between the roller and the stud bolt was calculated considering a critical brush shaft speed and structural safety under operating conditions. The flow chart for the optimal design of the clamp load using theoretical analysis and FEA is shown in Figure 6.

The theoretical model to analyse sliding, which consists of the driving roller, driven roller, clamp and stud bolt, is illustrated in Figure 7. The stud bolt and the driven roller rotate at the velocity of 30 rpm by rotating motion of the driving roller. The driving and driven rollers have the same radius (r) of 32.5 mm, and the materials of the rollers and stud bolt are engineering rubber (Mangle star) and chromium-molybdenum steel (SCM4), respectively.

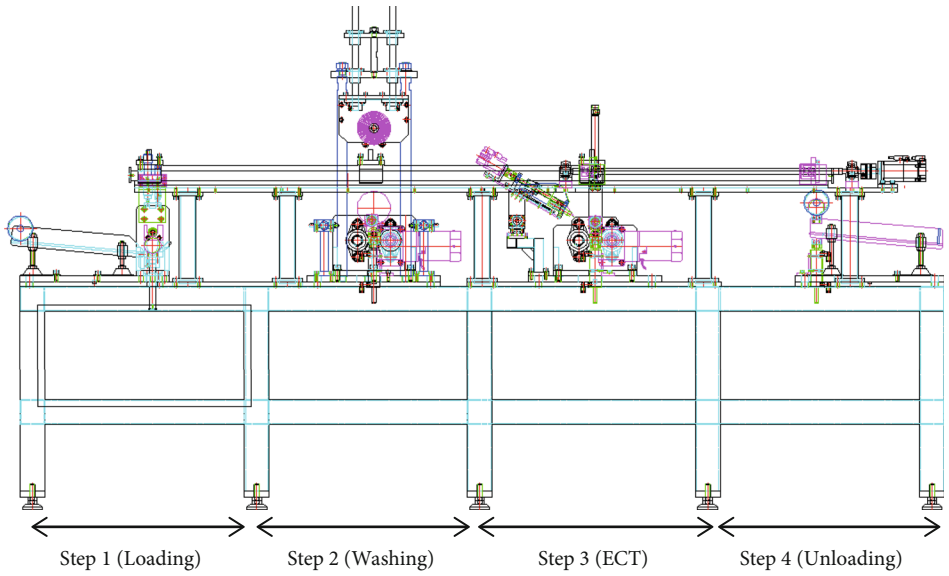

Figure 4: Equipment for washing and nondestructive inspection of stud bolt.

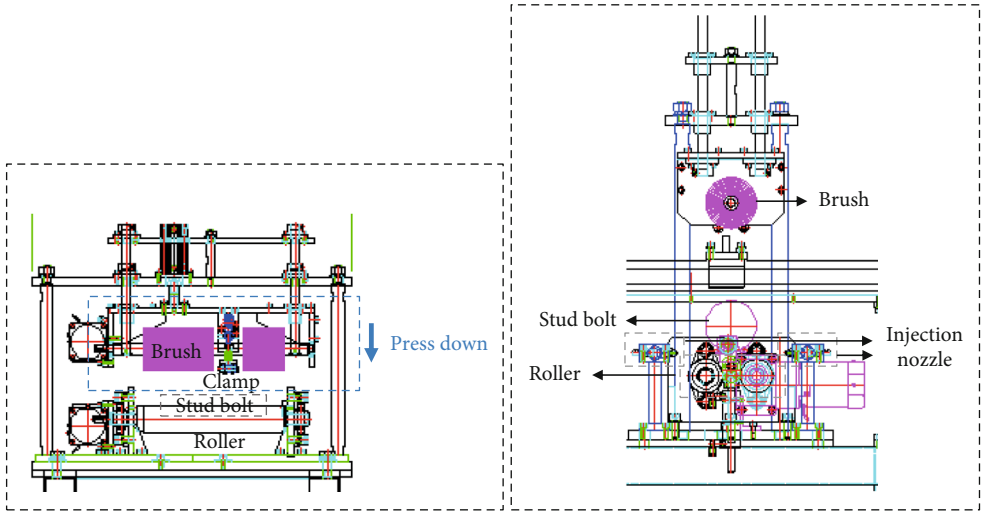

Figure 5: Detailed view of washing part (step 2): (a) side view and (b) front view.

The torque of the driving shaft, T_r, (kg·mm) was calculated by using Equation (1), where H and N are the power (kW) of motor and rotational velocity (rpm), respectively [15]. The torque of the driven shaft (T_f) derived from a clamp load is expressed with a friction force (F_f) as shown in Equation (2). The friction force (F_f) is determined on the condition that T_f is the same as T_r. The power (H) is given by 0.09 kW in the actual field, and the theoretical friction force (F_f) exerted between the stud bolt and the driven roller was 881.02 N.

$$T_r = 974{,}000 \times \frac{H}{N}, \tag{1}$$

$$T_f = F_f \times r. \tag{2}$$

FEA was performed to obtain a clamp load (F_c) to prevent sliding, which produces the theoretical friction force of 881.02 N, by using commercial software, ANSYS Workbench. The FEA model consisting of the driving roller, driven roller, clamp, and stud bolt was generated by using SpaceClaim, as shown in Figure 8. Analysis of the mesh quality shows that the minimum value for orthogonal quality, which should not fall below 0.05, is 0.24, and the maximum value for skewness, which should not exceed 0.98, is 0.84, so it is considered that the used mesh is proper.

The material properties of each component shown in Table 1 were used, and the lubricated friction coefficient of the roller to the stud bolt was applied as 0.07, which is a general value used in between the steel and the engineering rubber [16, 17], and that of the bolt to the clamp was applied as 0.16 [18, 19].

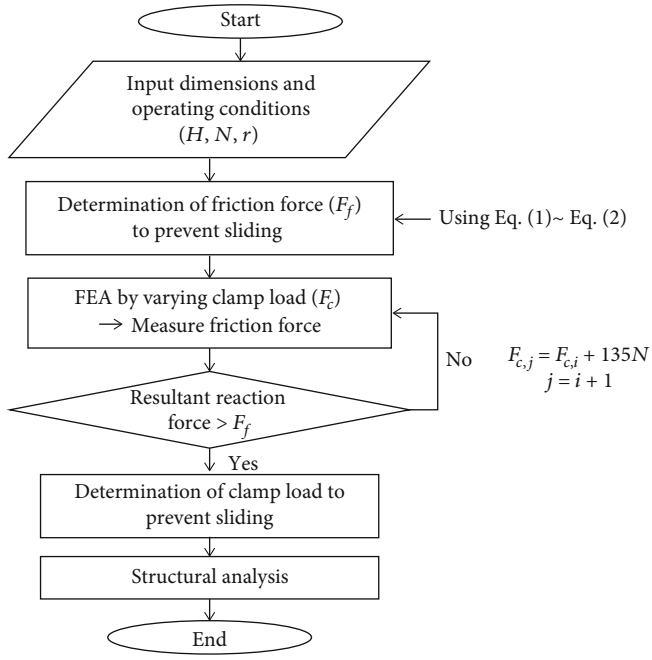

Figure 6: Flow chart for the optimal design of clamp load to prevent sliding between the roller and stud bolt.

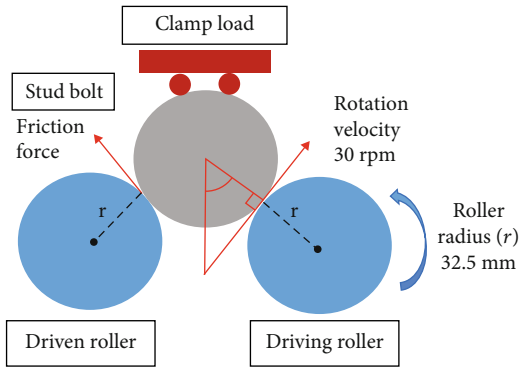

Figure 7: Theoretical analysis model to predict sliding between the roller and the stud bolt.

The earth's gravity of 9.8 m/s^2 was adopted to consider the self-weight of the components. Cylindrical support condition was applied on the shafts of the rollers. Deformation and movement in the axial and tangent directions were constraints, and those in the radial direction were allowed [20]. The friction force in Figure 9 is resultant of the reaction forces in the x-axis and y-axis (F_x, F_y), which are applied to the contact surfaces, so structural analyses were conducted until the resultant reaction force is equal to the theoretical friction force (881.02 N), by increasing the clamp load starting from 135 N at the interval of 135 N. Based on the FEA results listed in Table 2, when a clamp load of 675 N was imposed, the resultant reaction force of 881.88 N, which is the closest value of the theoretical friction force (881.02 N), was obtained as shown in Figure 10, so the optimal clamp load to prevent sliding was determined as 675 N.

To verify the structural safety of the automatic equipment used in the washing process (step 2), which undergoes the most severe external conditions, structural analysis of the washing device was performed. The FEA model including the clamp, brush, driving/driven rollers, and air/washing liquid injection nozzles was created as shown in Figure 11. The clamp, roller, stud bolt, and injection nozzles where the external loads were imposed were filled with fine mesh, which results in an interior refinement area with finer mesh sizes and coarse regions around it, and 406,216 elements were generated. The bottom surface was fully fixed, and the cylindrical support condition was given to the brush shaft and driving/driven roller (axial and tangent directions: fixed, the radial direction: free), as shown in Figure 12(a). The driving roller shaft and brush shaft rotated at 30 rpm and 300 rpm, respectively. The air injection and fluid washing liquid injection pressures were 3 and 8 bar, respectively, and the clamp load of 675 N was imposed as shown in Figure 12(b). The lubricated friction coefficient of the roller to the stud bolt (0.07) and that of the bolt to the clamp (0.16) was the same as the above FEA, and that of the support plate to the rotating elements (driving roller and brush shaft) (0.05) was applied [21, 22]. According to the results of the structural analysis shown in Figure 13, the maximum equivalent stress of 42.8 MPa occurred at the support plate end, which contacts with the brush shaft, because it was affected by the rotation speed, clamp load, and deflection of the brush shaft. The maximum value was much lower than the yield strength of 215 MPa, so it is considered that the equipment is safe under the operating conditions.

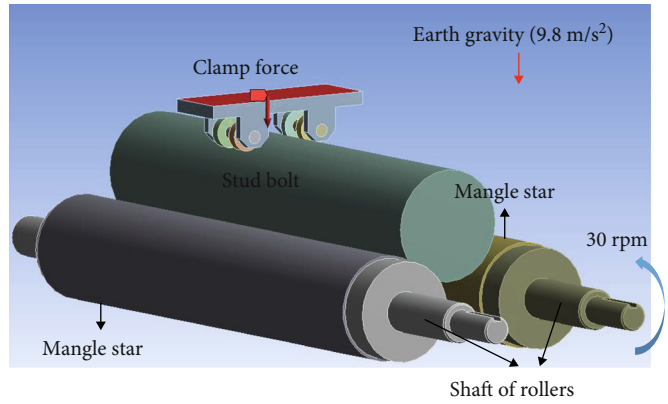

Figure 8: FEA model to obtain the optimal clamp load.

Table 1: Material properties of each component.

	Shaft, clamp, and beam (STS304)	Stud bolt (SCM4)	Engineering rubber (Mangle star)
Yield strength	215 MPa	420 MPa	21.6 MPa
Tensile strength	505 MPa	655 MPa	—
Young's modulus	193 GPa	190 GPa	0.003 GPa
Poisson's ratio	0.29	0.27	0.48

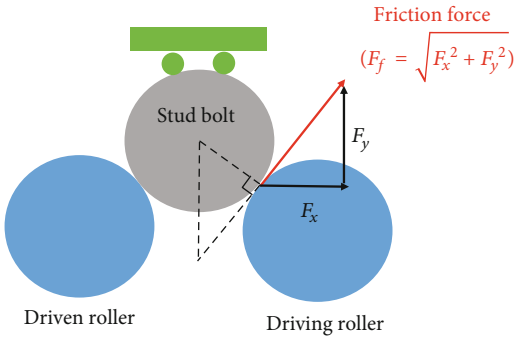

Figure 9: Component of friction force.

Table 2: Reaction forces at the contact area according to the clamp load (unit: N).

Clamp load	Reaction force (x -direction)	Reaction force (y -direction)	Resultant reaction force
135	-341.5	15.582	341.82
270	-476.49	22.053	476.48
405	-611.49	23.917	611.96
540	-746.49	25.189	746.92
675	-881.49	26.249	881.88

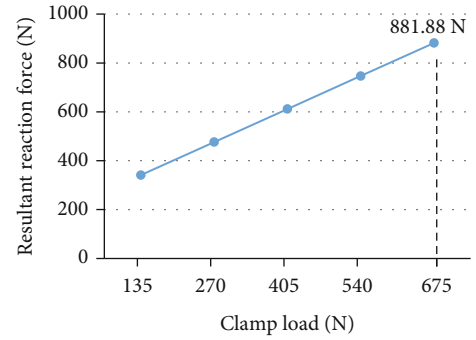

Figure 10: Optimal resultant reaction force (friction force).

4. Design of Optimal Condition to Improve Washing Efficiency

The prototype of the automatic equipment was manufactured. The entire structural design is shown in Figure 14(a), and details of the washing part (step 2) and the nondestructive inspection part (step 3) are shown in Figures 14(b) and 14(c). To validate the optimal clamp load (675 N) obtained from theoretical analysis, the operating tests with increasing the clamp load according to Table 2 were carried out as shown in Figure 15, and the test was repeated 10 times to ensure high accuracy of the results. The minimum clamp load not to allow sliding was about 628 N, which is in good agreement with the theoretical clamp load of 675 N (within 7.5% error).

To conduct the optimal design of washing conditions to obtain a high washing rate (response) within the given time of 30 s, Taguchi's method was applied by using the Minitab program. The control factors relating to the washing rate were determined based on the machine specification and the worker's field experience as follows: washing liquid injection pressure from 2 to 5 bar, air injection pressure from 3 to 7 bar, the rotation speed of the brush shaft from 90 to 360 rpm, and washing time from 5 to 30 s. The orthogonal array was generated as three levels (L_9 (3^4)) as shown in Table 3. As the noise factors, the new brush and the old brush, which had been used in the field for 1 year, were used in the experiments.

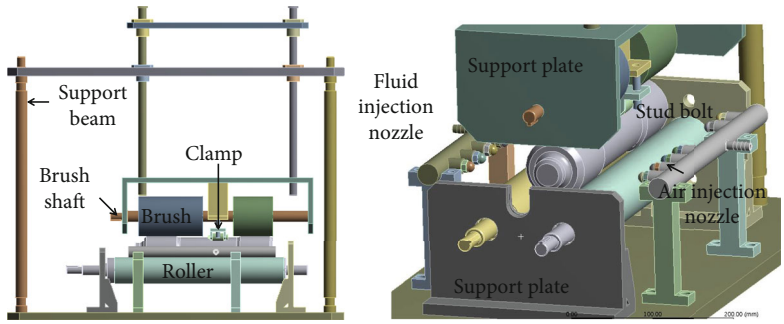

Figure 11: 3D modelling for structural analysis.

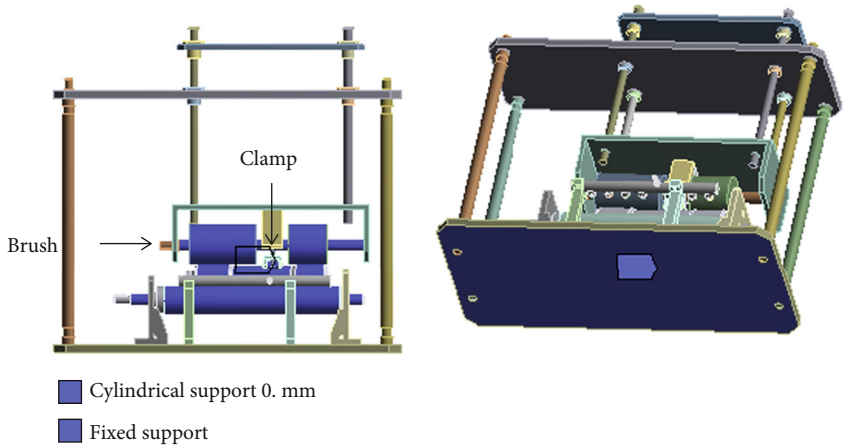

(a)

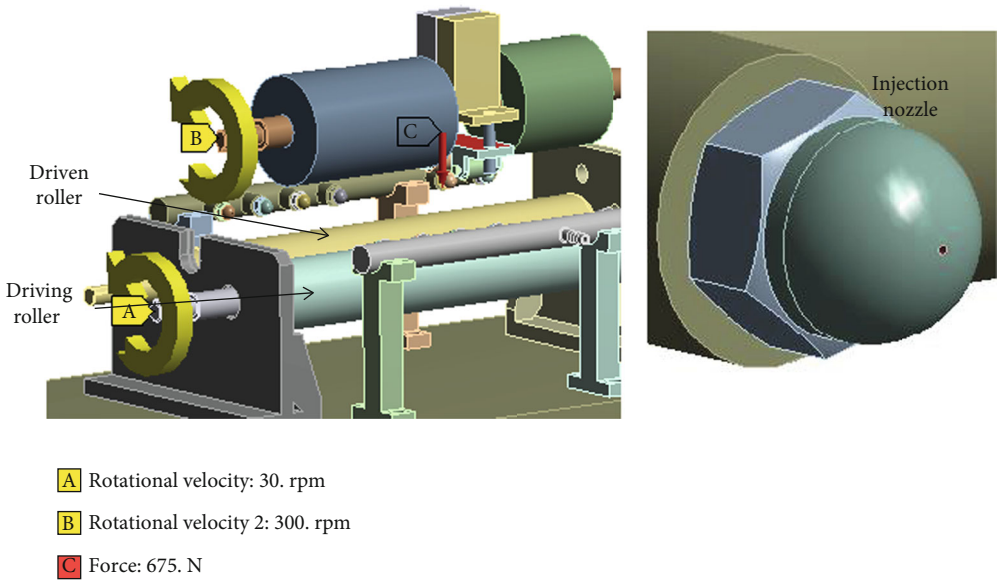

(b)

Figure 12: Boundary and load conditions: (a) boundary conditions and (b) load conditions.

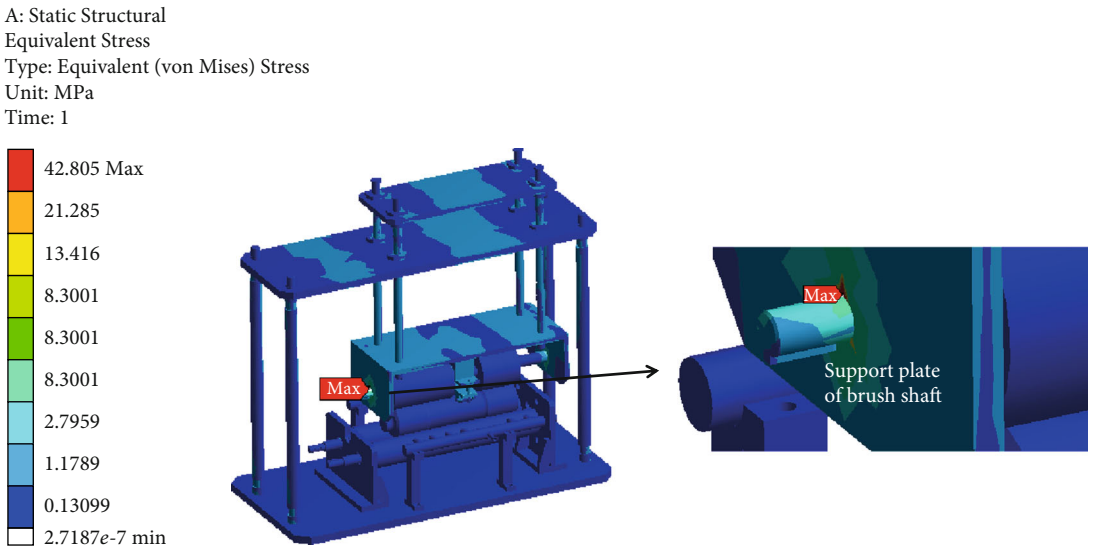

Figure 13: Result of structural analysis of the equipment.

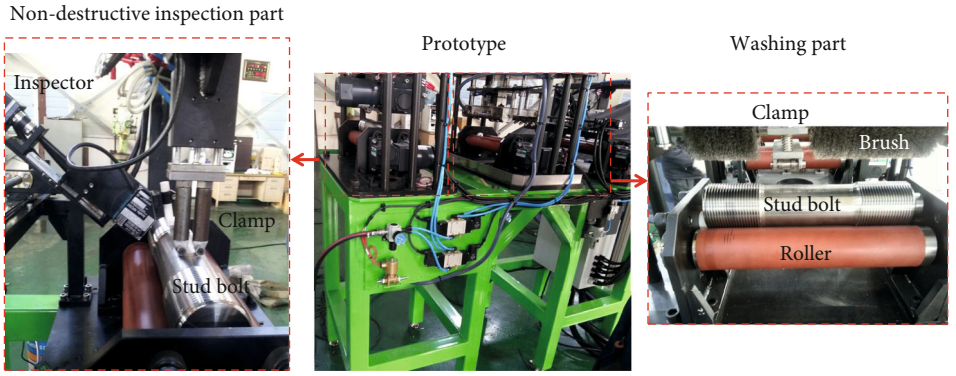

Figure 14: The prototype of the automatic equipment.

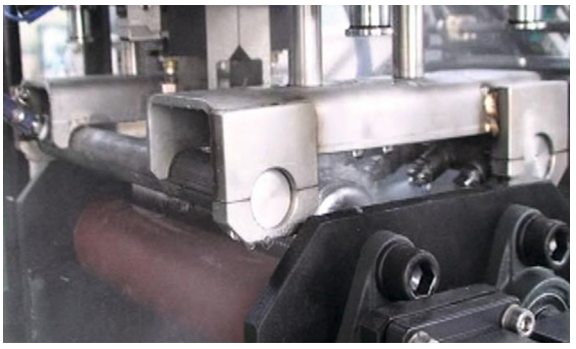

Figure 15: Operating test to validate the clamp load.

The washing tests were performed according to the orthogonal array, and the washing rate for each experiment was calculated using Equation (3), by comparing the bolt weights before and after washing, and the results are listed

Table 3: Orthogonal array (L_9 (3^4)).

No.	Control factor			
	Washing liquid injection pressure (bar)	Air injection pressure (bar)	Rotational speed of brush shaft (rpm)	Washing time (s)
1	2	3	90	5
2	2	5	180	15
3	2	7	360	30
4	3	3	180	30
5	3	5	360	5
6	3	7	90	15
7	5	3	360	15
8	5	5	90	30
9	5	7	180	5

Table 4: Washing rate according to the orthogonal array.

No.	Initial bolt weight (g)	Bolt weight before washing (g)	Bolt weight before washing (g)	Washing rate (%)
1	5228.1	5234.4	5229.9	71.4
2	5228.1	5235.9	5228.6	93.6
3	5228.1	5236.1	5228.4	96.3
4	5242.9	5250.8	5243.2	96.2
5	5228.1	5236.3	5228.7	92.7
6	5228.1	5237.1	5230.0	78.9
7	5242.9	5252.4	5243.2	96.8
8	5242.9	5252.6	5245.0	78.4
9	5228.1	5237.5	5229.8	81.9

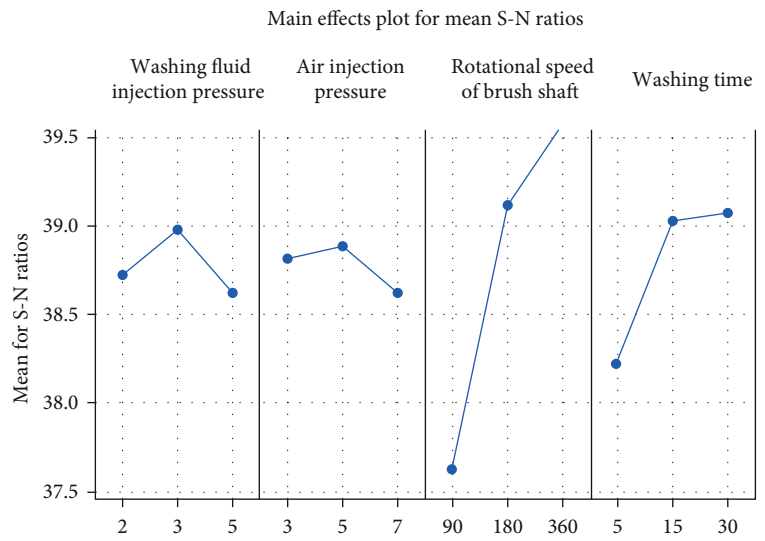

Figure 16: Mean S-N ratio graph.

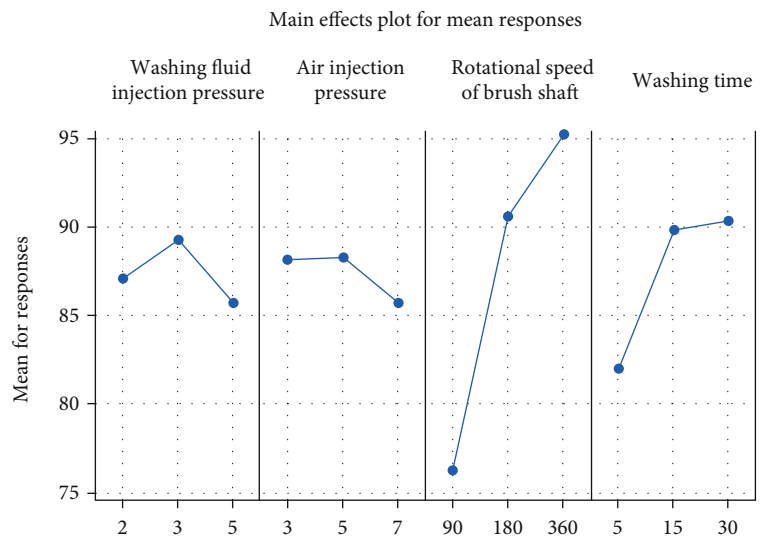

Figure 17: Mean response graph.

Table 5: Analysis of variance.

(a) Analysis of variance for S-N ratios

Level	S-N ratio			
	Washing liquid injection pressure	Air injection pressure	Rotational speed of brush shaft	Washing time
1	38.72 (2 bar)	38.82 (3 bar)	37.63 (90 rpm)	38.23 (5 s)
2	**38.98 (3 bar)**	**38.88 (5 bar)**	39.12 (180 rpm)	39.03 (15 s)
3	38.62 (5 bar)	38.63 (7 bar)	**39.58 (360 rpm)**	**39.07 (30 s)**
Variance	0.04	0.02	1.04	0.23
Rank	3	4	1	2

(b) Analysis of variance for responses

Level	Response			
	Washing liquid injection pressure	Air injection pressure	Rotational speed of brush shaft	Washing time
1	87.10 (2 bar)	88.13 (3 bar)	76.23 (90 rpm)	82.00 (5 s)
2	**89.27 (3 bar)**	**88.23 (5 bar)**	90.57 (180 rpm)	89.77 (15 s)
3	85.70 (5 bar)	85.70 (7 bar)	**95.27 (360 rpm)**	**90.30 (30 s)**
Variance	3.24	2.05	98.37	21.60
Rank	3	4	1	2

in Table 4.

$$1 - \left(\frac{\text{Initial bolt weight} - \text{Bolt weight after washing}}{\text{Initial bolt weight} - \text{Bolt weight before washing}}\right) \times 100. \quad (3)$$

The mean S-N (signal-to-noise) ratios with the characteristic that the larger is the better and the mean responses (washing rates) were plotted in Figures 16 and 17, respectively, and their analyses of variances were conducted to investigate the effect of the control factors on the washing rate as shown in Table 5.

It was found that the rotation speed of the brush shaft, which has the biggest variance of S-N ratio (1.04), has the largest impact on deviation of the S-N ratio, and the remaining control factors are as follows: washing time (0.23), washing liquid injection pressure (0.04), and air injection pressure (0.02), as shown in Table 5(a). Also, the rotation speed of the brush shaft has the biggest variance of response (98.37), which has the largest impact on washing rate. The order of the remaining control factors are as follows: washing time (21.60), washing liquid injection pressure (3.24), and air injection pressure (2.05), as shown in Table 5(b). To minimize variation and to maximize washing rate, the control factors to maximize the mean S-N ratio and the mean response are selected as follows: washing liquid injection pressure of 3 bar, air injection pressure of 5 bar, the rotation speed of the brush shaft of 360 rpm, and washing time of 30 s.

To verify the above suggested control factors, 10 times repeated washing tests were performed, and the mean washing rate of 97.7%, which is higher than the requirement in the field (95%) and the results in Table 4, was obtained as shown in Table 6. Analysis of variations was conducted as shown in Table 7, and 40.19 of S-N ratio and 100% of washing rate were obtained. This shows the big improvements compared to No. 1 in Table 3 with level 1 (2 bar, 3 bar, 90 rpm, and 5 s), which has the variations of 37.07 and 71.4%, respectively, so the optimal design method and optimal control factors were verified.

5. Conclusions

This study developed the automatic equipment for washing the sludge and the nondestructive inspection of stud bolt used in low-pressure steam turbines in the power plants. The optimal clamp load to prevent sliding between the roller and the stud bolt was derived, and the structural safety of the equipment was verified under the operating conditions. An optimal design of washing condition was performed to improve the washing rate of the stud bolt. The summaries are as follows.

(1) The integrated automatic equipment by combining the washing part and the inspection part was devised. It consists of driving/driven rollers, clamp, brush, shaft, and injection nozzles and has four stages. Step 1 is the loading process, and in step 2, the brush roller cleans sludge, and two injection nozzles spray air and washing liquid, respectively, to remove the remaining sludge. In step 3, the nondestructive inspection of the stud bolt is conducted, and finally, the stud bolt is unloaded in step 4

(2) The optimal clamp load of 628 N to prevent sliding between the roller and the bolt was obtained from the operating test, and this value is a good agreement

Table 6: Washing rate applying the optimal control factors.

Initial bolt weight (g)	Bolt weight before washing (g)	Bolt weight after washing (g)	Washing rate (%)
5228.1	5237.0	5228.3	97.7

Table 7: Washing rate applying the optimal control factors.

	Washing liquid injection pressure 3 bar	Air injection pressure 5 bar	Rotational speed of brush shaft 360 rpm	Washing time 30 s
Mean S-N ratio	40.12			
Mean response	100.0			

(7.5% error) with the clamp load of 675 N obtained from the theoretical analysis and FEA

(3) The structural analysis result of the washing device showed that the maximum equivalent stress of 42.8 MPa occurring at the support plate was lower than the yield strength (215 MPa), which means that the equipment is safe under the operating conditions

(4) Based on Taguchi's method, the best washing rate (97.7%) was derived when the process variables are as follows: washing liquid injection pressure of 3 bar, air injection pressure of 5 bar, rotation speed of the brush shaft of 360 rpm, and washing time of 30 s

By applying the automatic equipment and the optimal washing condition, a considerable shortening of working hours and labor saving can be accomplished and the overall time required for an annual inspection of a nuclear power plant can be reduced.

Data Availability

The data used to support the findings of this study are included within the article.

Conflicts of Interest

The author declares that there are no competing interests regarding the publication of this paper.

Acknowledgments

This work was supported by the Youngsan University Research Fund of 2020.

References

[1] R. Laycock and T. H. Fletcher, "Independent effects of surface and gas temperature on coal fly ash deposition in gas turbines at temperatures up to 1400 C," *Journal of Engineering for Gas Turbines and Power*, vol. 138, no. 2, 2016.

[2] J. Collin, R. Jones, J. Luszcz et al., *"Low-pressure sludge removal method and apparatus using coherent jet nozzles," U.S. Patent No. 7,967,918*, U.S. Patent and Trademark Office, Washington DC, 2011.

[3] G. Totten, R. Shah, and D. Forester, *Fuels and Lubricants Handbook: Technology, Properties, Performance, and Testing*, ASTM International, West Conshohocken, PA, 2nd edition, 2019.

[4] D. Sakthivel, R. Dharunkumarasamy, L. Karthikeyan, S. P. Kumar, and B. Surya, "Experimental investigation on brick manufacturing by using sludge & pulp production residue," *International Research Journal of Engineering and Technology*, vol. 6, no. 3, pp. 266–274, 2019.

[5] Q. Wang, W. Wei, Y. Gong et al., "Technologies for reducing sludge production in wastewater treatment plants: state of the art," *Science of the Total Environment*, vol. 587, no. 1, pp. 510–521, 2017.

[6] Y. Muraguchi, *"Device for cleaning cylindrical objects, such as bolts," U.S. Patent No. 5,005,244*, U.S. Patent and Trademark Office, Washington DC, 1991.

[7] F. Linna, S. Min, L. Zhaodong, G. Mingfei, and H. Zongren, "Research and development on the cleaning machine for reactor pressure vessel bolt," *China Nuclear Power*, vol. 7, no. 1, pp. 223–227, 2014.

[8] T. Shindo, K. Shigehiro, K. Okada, M. Ito, and S. Abe, "Development of remote controlled stud bolt handling device," *Design & Analysis*, vol. 2, pp. 1263–1270, 1989.

[9] J. M. Saurer, *"Bolt cleaning system," U.S. Patent No. 6,983,508*, U.S. Patent and Trademark Office, Washington DC, 2006.

[10] K. Smart and B. Monteith, *Wheel stud cleaning device*, U.S. Patent No. 11/287,261, U.S. Patent and Trademark Office, Washington, DC, 2006.

[11] E. G. Gibson Sr., *"Cleaning device," U.S. Patent No. 3,435,479*, U.S. Patent and Trademark Office, Washington DC, 1969.

[12] H. W. Xie, Y. F. Zhang, and Y. Zhang, "Numerical simulation and experimental study of flue gas cleaning in waste incineration power plants," *Proceedings-Chinese Society Of Electrical Engineering*, vol. 28, no. 5, p. 17, 2008.

[13] H. Lee, Y. Park, S. Lee, and H. Jeong, "Preliminary study on the effect of spray slurry nozzle in CMP for environmental sustainability," *International Journal of Precision Engineering and Manufacturing*, vol. 15, no. 6, pp. 995–1000, 2014.

[14] M. Mofidi, B. Prakash, B. N. J. Persson, and O. Albohr, "Rubber friction on (apparently) smooth lubricated surfaces," *Journal of Physics: Condensed Matter*, vol. 20, no. 8, article 085223, 2008.

[15] G. B. Song, W. B. Bae, Y. J. Jo, S. M. Hwang, and J. R. Jo, *Mechanical Engineering Design*, KyoBo, 3rd edition, 2004, ISBN 9788993995718 (8993995710).

[16] C. L. Dong, C. Q. Yuan, X. Q. Bai, Y. Yang, and X. P. Yan, "Study on wear behaviors for NBR/stainless steel under sand water-lubricated conditions," *Wear*, vol. 332, pp. 1012–1020, 2015.

[17] D. P. Manning, C. Jones, F. J. Rowland, and M. Roff, "The surface roughness of a rubber soling material determines the coefficient of friction on water-lubricated surfaces," *Journal of Safety Research*, vol. 29, no. 4, pp. 275–283, 1998.

[18] R. C. Hibbeler, *Engineering Mechanics: Statics*, Pearson Education India, Prentice Hall, 11th edition, 2007, ISBN 978-0-13-127146-3.

[19] S. Little, W. Robert, J. D. Inman, and D. Balint, *Engineering Mechanics*, Thomson, 2007, ISBN 978-0-495-29610-2.

[20] K. L. Lawrence, *ANSYS workbench tutorial release 14*, SDC publications, 2012, ISBN-13: 978-1585037544.

[21] R. K. Upadhyay and L. A. Kumaraswamidhas, "Bearing failure issues and corrective measures through surface engineering," in *Handbook of Materials Failure Analysis*, pp. 209–233, Butterworth-Heinemann, 2018.

[22] C. H. Simmons, N. Phelps, and D. E. Maguire, *Manual of Engineering Drawing*, Butterworth-Heinemann, 4th edition, 2012.